Random Wave Model in theory and experiment

Ulrich Kuhl

Philipps Universität Marburg

Fachbereich Physik, Philipps-Universität Marburg, D-35032 Marburg, Deutschland

Maribor, 23 - 27 February 2009

ulrich.kuhl@physik.uni-marburg.de

Literature on Quantum Chaos

- H.-J. Stöckmann, Quantum Chaos - An Introduction
- F. Haake, Quantum Signatures of Chaos
- M. C. Gutzwiller, Chaos in Classical and Quantum Mechanics
- M. L. Mehta, Random Matrices
- B. Eckhardt, Quantum mechanics of classically non-integrable systems, Phys. Rep. 163, 205 (1988)
- O. Bohigas in: Proc. Les Houches Summer School on Chaos and Quantum Physics
- T. Guhr, A. Müller-Groeling, and H. A. Weidenmüller, Random matrix theories in quantum physics: common concepts, Phys. Rep. 299, 189 (1998)
- M.V. Berry, in: M.J. Gianonni, A. Voros, J. Zinn-Justin (Eds.), Chaos and Quantum Physics

Literature on Classical Chaos

- A. J. Lichtenberg and M. A. Liebermann. Regular and Stochastic Motion
- E. Ott, Chaos in Dynamical Systems
- H.G. Schuster, Deterministic chaos: An introduction
- P. Cvitanovic et al, Classical and Quantum Chaos, (www.nbi.dk/ChaosBook/)

Papers

- M. S. Longuet-Higgins, Phil. Trans. R. Soc. Lond. A 249, 321 (1957)
- M. S. Longuet-Higgins, Proc. R. Soc. Lond. A 246, 99 (1958)
- M. V. Berry, J. Phys. A 10 (1977) 2083)
- K. J. Ebeling, Optica Acta 26, 1345 (1979)
- M. V. Berry and M. R. Dennis, Proc. R. Soc. Lond. A 456, 2059 (2000).
- Y.-H. Kim, M. Barth, U. Kuhl, and H.-J. Stöckmann, Prog. Theor. Phys. Suppl. 150, 105 (2003)
- J. D. Urbina and K. Richter, J. Phys. A 36, L495 (2003)
- U. Kuhl, Eur. Phys. J. Special Topics 145, 103 (2007)
- M. R. Dennis, Eur. Phys. J. Special Topics 145, 191 (2007)
- S. Tomsovic, D. Ullmo, and A. Bäcker. Phys. Rev. Lett. 100, 164101 (2008)
- R. Höhmann, U. Kuhl, H.-J. Stöckmann, J. D. Urbina, and M. Dennis, Phys. Rev. E 79, 016203 (2009)

Classical billiards I

There exist only a few billiards with integrable dynamics:

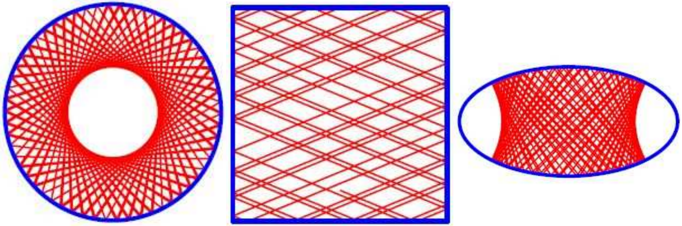

There are some with fully chaotic dynamics:

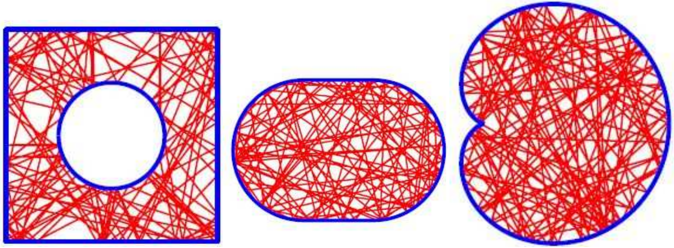

- Mostly dynamics have a mixed phase space

Limaçon billiard ($\rho = z + \lambda z^2, z \in C, |z| = 1$) and Poincaré map

$\lambda = 0.00$

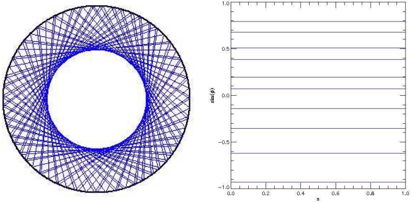

$\lambda = 0.05$

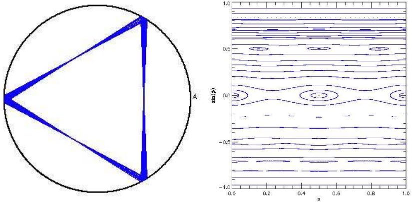

$\lambda = 0.20$

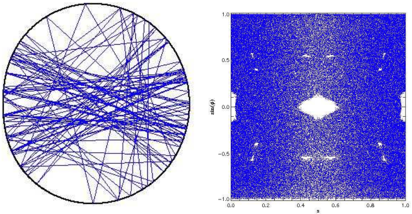

$\lambda = 0.50$

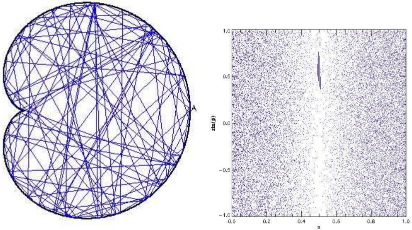

Hierarchy of classical chaos

Name	Definition	Example
Recurrent	Trajectory reoccurs infinitely often to its neighborhood	All Hamiltonian systems, with a finite phase space (not chaotic).
Ergodic	time average $\Leftrightarrow$ phase space average	$x_{n+1} = (x_n + b) \bmod 1$ b : irrational (not necessarily chaotic)
Mixing	Correlation function declines for infinitely long times	always chaotic, cat map ($x_{n+1} = (x_n + y_n) \bmod 1$, $y_{n+1} = (x_n + 2y_n) \bmod 1$)
K-system	Nearly all trajectories are exponentially separated	Stadium billiard (not C!), cat map
C-System	The system is hyperbolic in all phase space points	Billiard with constant negativ curvature
Bernoulli-system	System with full symbolic dynamics and finite number of symbols and a full shift	Bernoulli-shift-map

Classical waves

Experiments can be performed with different classical waves

- microwaves

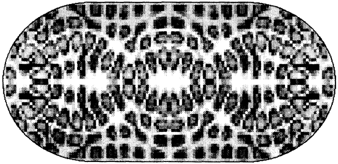

- acoustics in solids

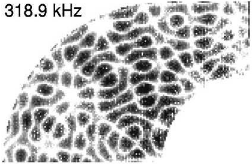

- light

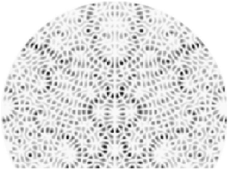

- water surface waves

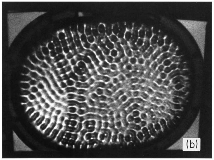

- ultrasound in water

Microwave resonators

- cylindrical symmetry in z-direction
  z-component can be separated
- transverse magnetic (TM) modes
  $\vec{E} = (0, 0, E_z(x, y, z))$
- metallic top and bottom plates
  cut-off frequency $\nu_c = c/2h \Rightarrow E_z(x, y)$
- two-dimensional Helmholtz equation.

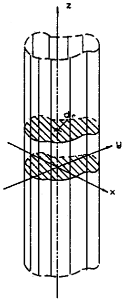

Microwave resonators

- cylindrical symmetry in z-direction
  z-component can be separated
- transverse magnetic (TM) modes
  $\vec{E} = (0, 0, E_z(x, y, z))$
- metallic top and bottom plates
  cut-off frequency $\nu_c = c/2h \Rightarrow E_z(x, y)$
- two-dimensional Helmholtz equation.

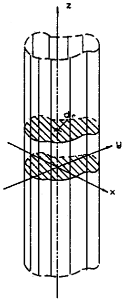

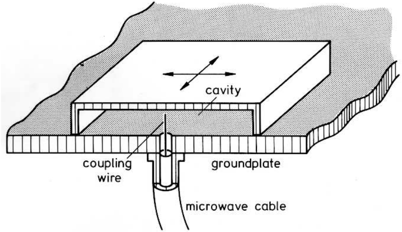

Typical set-up

Frequency: 1 – 20 GHz
Wave length: 1.5 – 30 cm

Microwaves versus quantum mechanics

There is a one-to-one correspondence between the stationary Schrödinger equation

$$-\frac{\hbar^2}{2m}\left(\frac{\partial^2}{\partial x^2}+\frac{\partial^2}{\partial y^2}\right)\psi_n = E_n\psi_n$$

with the boundary condition $\psi_n|_S = 0$ (billiard), and the two-dimensional Helmholtz equation

$$-\left(\frac{\partial^2}{\partial x^2}+\frac{\partial^2}{\partial y^2}\right)E_n = k_n^2 E_n.$$

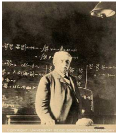

(E_n: electric field strength of z-component)

In quasi-two-dimensional microwave billiards even the electromagnetic and the quantum mechanical boundary conditions are equivalent.

Advantages of microwave experiment

Real quantum systems:

- antidot structures (Weiss *et al.* 1991)
- mesoscopic billiards (Marcus *et al.* 1992)
- quantum corrals (Crommie *et al.* 1993)
- tunnelling barriers (Fromhold *et al.* 1994)

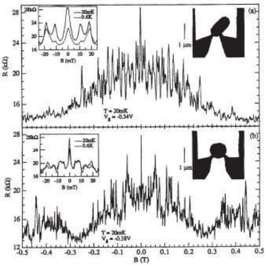

Magnetoresistance of quantum dots

Aspects of microwave billiards:

- corresponds to mesoscopic physics
- daily-life sizes, parameters are easy to control
- no Coulomb interaction
- test bed for scattering theory (nuclear physics)
- commercial measurement equipment (VNA)

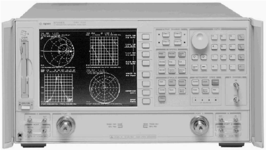

Husimi representation I

Example of a pulse as a projection on a Poincaré-Husimi function with minimal 'uncertainty':

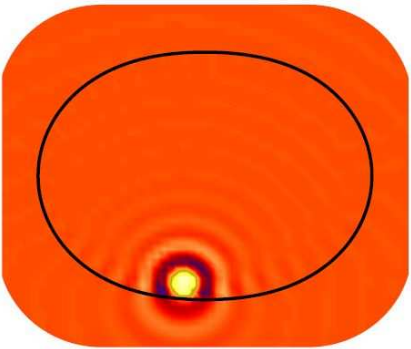

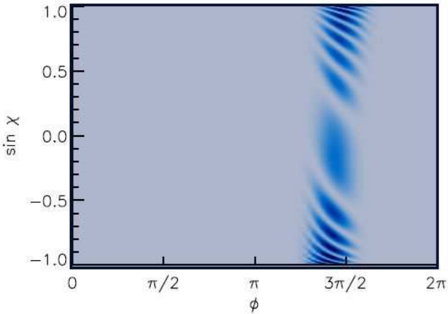

[R. Schäfer et al. NJP 8, 46 (2006)]

Husimi representation II

Classical Poincaré map vs. Poincaré-Husimi distribution of an open quadrupolar billiard (time averaged):

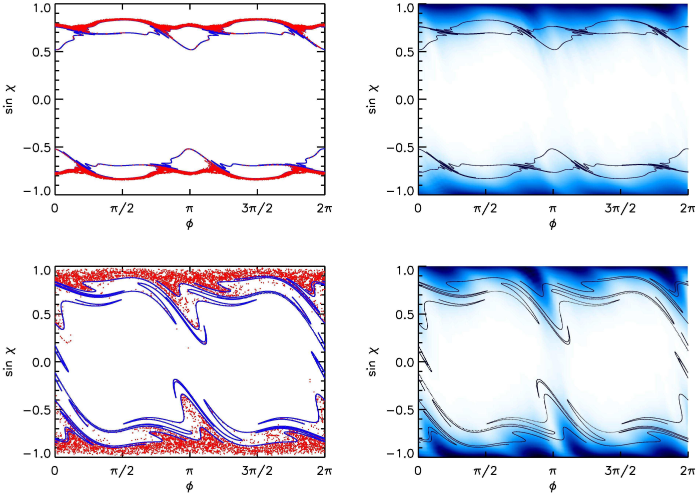

[R. Schäfer et al. NJP 8, 46 (2006)]

Random plane wave model

Which is an eigenfunction of a billiard and
which is a superposition of random plane waves?

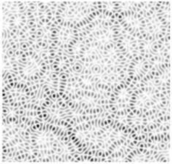

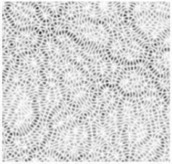

Random plane wave model

Which is an eigenfunction of a billiard and
which is a superposition of random plane waves?

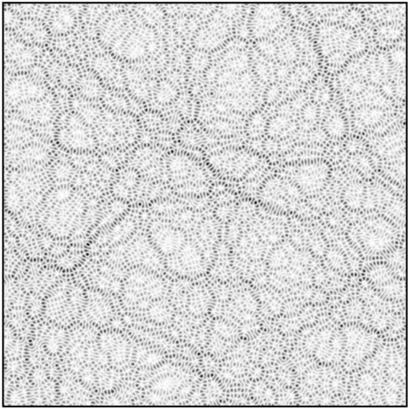

Random superposition
of plane waves

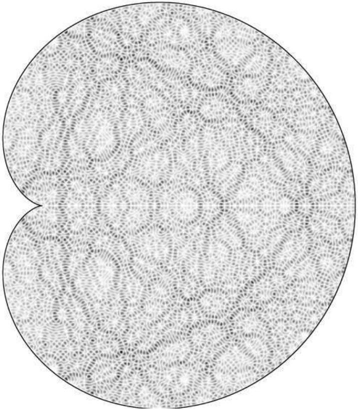

6000 eigenfunction
of a Limaçon billard

by courtesy of Arnd Bäcker

RWM - Distribution of ψ (closed system)

$$P(\psi) = \sqrt{\frac{A}{2\pi}} \exp\left(-\frac{A\psi^2}{2}\right)$$

where A : Area of the Billiard

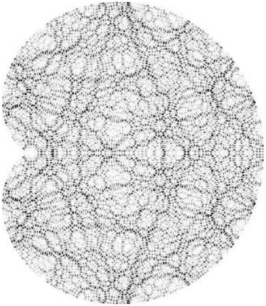

RWM - Distribution of ψ (closed system)

$$P(\psi) = \sqrt{\frac{A}{2\pi}} \exp\left(-\frac{A\psi^2}{2}\right)$$

where A : Area of the Billiard

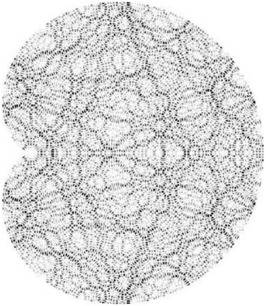

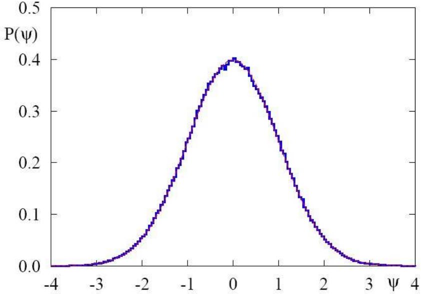

by courtesy of Arnd Bäcker

Light fiber (k direction)

Near field (left) and far field pattern of a D-shaped fiber.
The far field corresponds to a Fourier-transform of the nearfield and thus shows the distribution of $\vec{k}$ vectors.
[Doya et al. Phys. Rev. E 65, 056223 (2002)]

Intensity distribution (acoustic billiards)

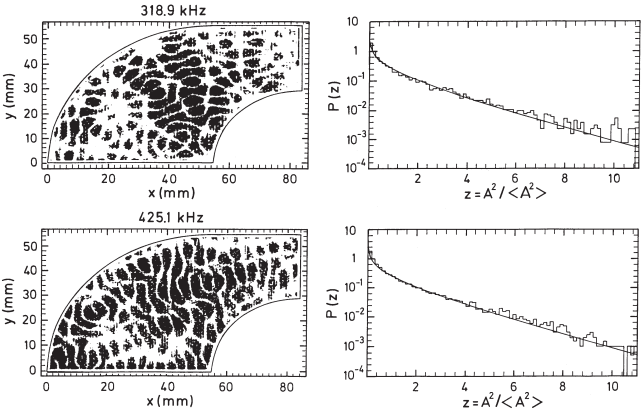

Vibration amplitude pattern for two eigenfrequencies of a plate of a quarter Sinai-stadium billiard (left column) and corresponding distribution function for the squared amplitudes. The solid line is a Porter-Thomas function.

[K. Schaadt, PhD-thesis, NBI, Copenhagen, 1997, H.-J. Stöckmann, Quantum Chaos - An Introduction (University Press, Cambridge, 1999).]

Partial width (microwaves)

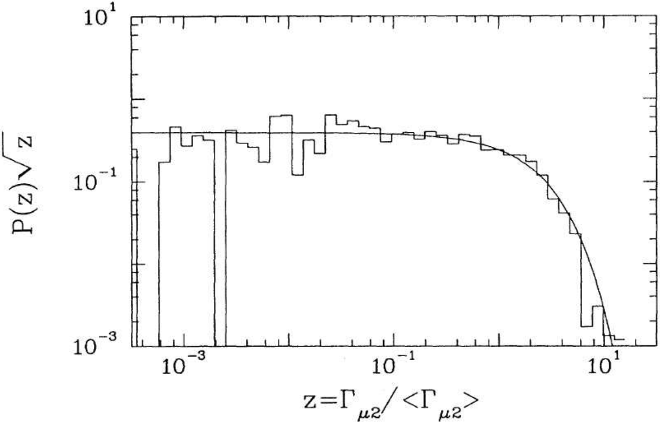

The partial width distribution of a two dimensional microwave cavity.

The solid line corresponds to a Porter-Thomas distribution.

[Alt et al. Phys. Rev. Lett. 74, 62 (1995)]

3-dimensional microwave billiard

- metallic sphere is moved inside the cavity
- Measured spectra as a function of frequency and sphere position.

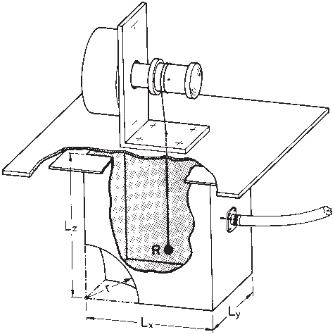

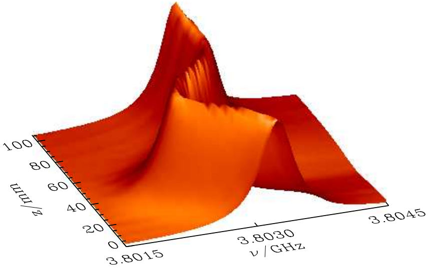

[Eckhardt et al. Europhys. Lett. 46, 134 (1999)]

Frequency shift distribution (3D billiard)

- 'Shift-eigenmode' ($\delta\nu \propto -2\vec{E}^2 + \vec{B}^2$)
- Distribution function of frequency shift $\Delta\nu$
- Assuming 6 independent Gaussian modes: $\Rightarrow$

$$P(\Delta\nu) = \frac{\sqrt{2}\alpha^2}{3\pi}|\Delta\nu| \exp\left(-\alpha\frac{\Delta\nu}{4}\right) K_1\left(\frac{3}{4}\alpha|\Delta\nu|\right)$$

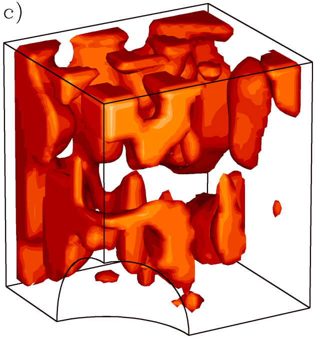

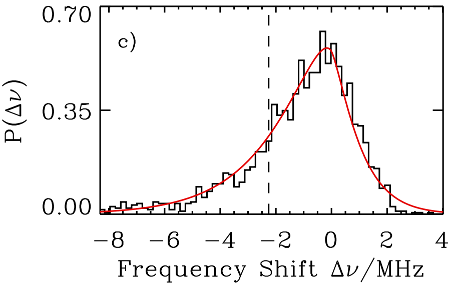

[Dörr et al. Phys. Rev. Lett. 80, 1030 (1998)]

Correlations function

- Correlation function C_Ψ and $C_{|\Psi|^2}$ for the stadium billiard (average over the 30 lowest eigenstates)

$$C_\Psi = \frac{1}{A} J_0(|k||r|)$$

$$C_{|\Psi|^2} = \frac{2}{3} \left(J_0(|k||r|)\right)^2 + \frac{1}{3}$$

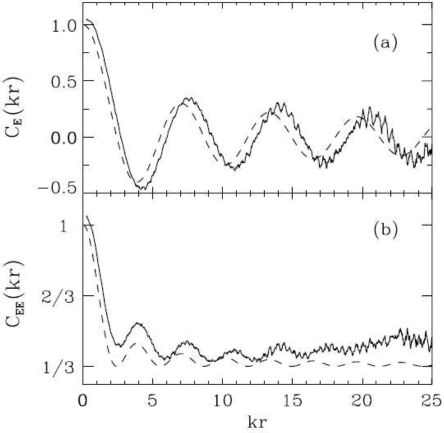

[Eckhardt et al. Europhys. Lett. 46, 134 (1999)]

Parametric dependence (global perturbation)

Corresponding level dynamics

Sketch of the Sinai billiards

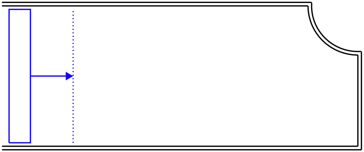

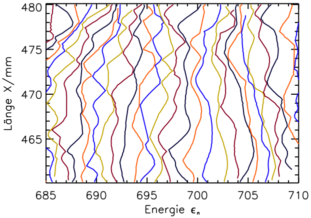

Global velocity distribution (Theory from RMT: Gaussian)

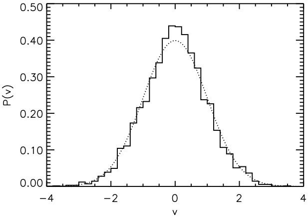

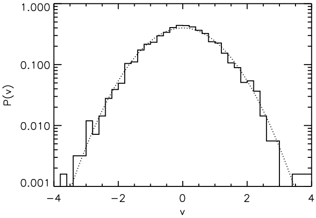

[Barth et al. Phys. Rev. Lett. 82, 2026 (1999), Bart et al. Ann. Phys. (Leipzig) 8, 733 (1999)]

Parametric dependencies (local perturbation)

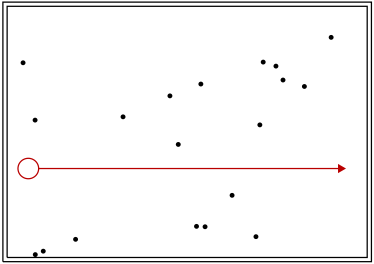

Rectangular billiard with scatterers, one is moved

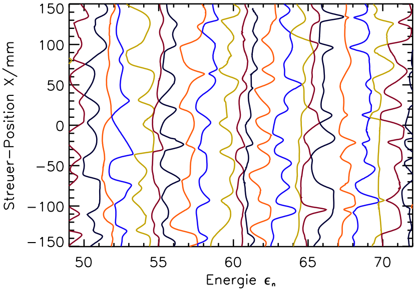

Dynamics of the normalized eigenvalues

[Barth et al. Phys. Rev. Lett. 82, 2026 (1999), Bart et al. Ann. Phys. (Leipzig) 8, 733 (1999)]

Local velocity distribution

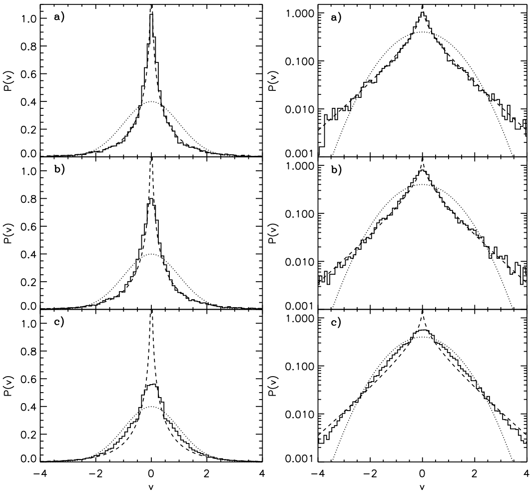

Local velocity distribution for different δ ranges:
$0.35 < \delta < 0.65$ (a), $1.4 < \delta < 2.6$ (b) bzw. $5.1 < \delta < 5.9$ (c)

[Barth et al. Phys. Rev. Lett. 82, 2026 (1999), Bart et al. Ann. Phys. (Leipzig) 8, 733 (1999)]

Velocity autocorrelation function (global)

- Global perturbation
- Dotted line corresponds to theory by Simons und Altshuler (RMT)

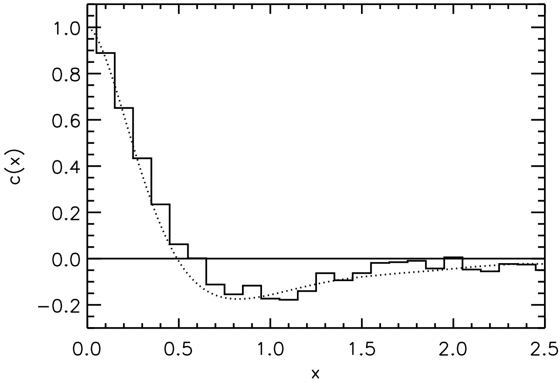

[Barth et al. Phys. Rev. Lett. 82, 2026 (1999), Bart et al. Ann. Phys. (Leipzig) 8, 733 (1999)]

Velocity autocorrelation (local)

- rescaled parameter kr
- for different δ ranges

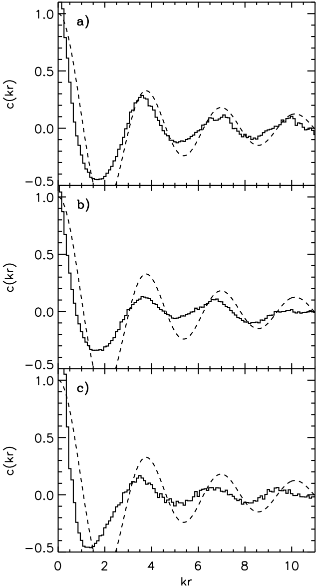

[Barth et al. Phys. Rev. Lett. 82, 2026 (1999), Bart et al. Ann. Phys. (Leipzig) 8, 733 (1999)]

Wavefunctions in open systems

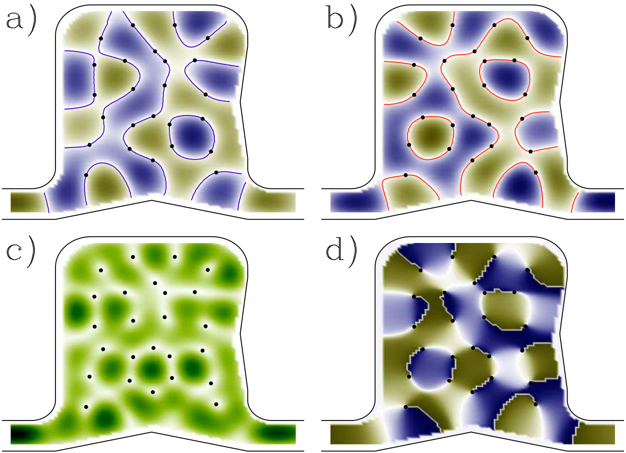

Real ψ_R (a), imaginary part ψ_I (b), modulus $|\psi|^2 = \psi_R^2 + \psi_I^2$ (c), and phase ϕ (d) of a wave function ψ at a frequency $\nu = 5.64$ GHz. Nodallines (for ψ_R und ψ_I) and nodal points (for $|\psi|^2$) are marked. White corresponds to the phase $\phi = 0$ in d).

[U. Kuhl, Eur. Phys. J. Special Topics 145, 103 (2007)]

Global phase rotation

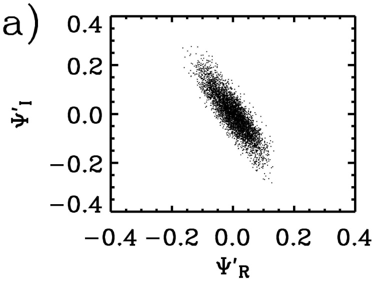

Imaginary- vs. real part of the wavefunction at a frequeny $\nu = 13.84\,$GHz. a) Directly measured and b) after a decorrelation via a global phase rotation, $\psi_\mathrm{R} + i\psi_\mathrm{I} = e^{-i\varphi_{g,0}}\,(\psi'_\mathrm{R} + i\psi'_\mathrm{I})$. $\varphi_{g,0}$ is a globale phase that comes in the experiment from the antenna and the channel.

[U. Kuhl, Eur. Phys. J. Special Topics 145, 103 (2007)]

Phase rigidity

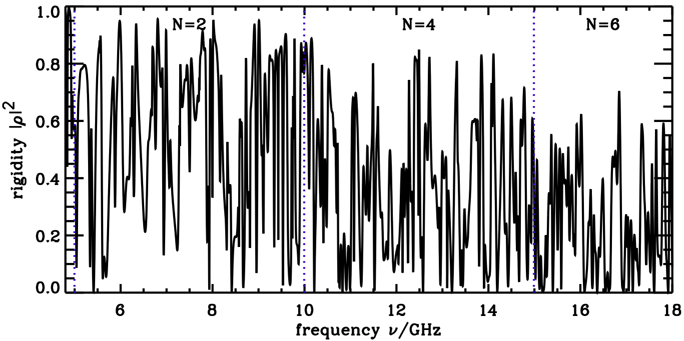

- Phase rigidity $|\rho|^2 = \left| \frac{\langle <\psi_R^2\rangle - \langle <\psi_I^2\rangle}{\langle <\psi_R^2\rangle + \langle <\psi_I^2\rangle} \right|^2$ as a function of frequency
- N corresponds to the number of open channels

[U. Kuhl, Eur. Phys. J. Special Topics 145, 103 (2007)]

Flow

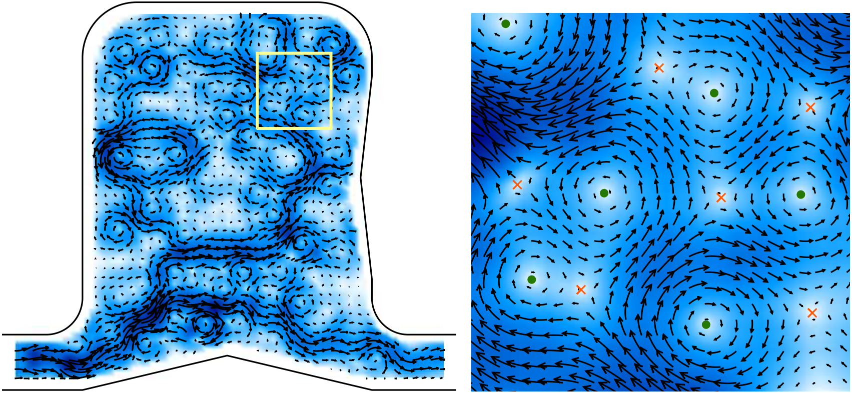

Probability current density $\vec{j}$. The color scale corresponds to the modulus $|j|$ and the arrows give the modulus and direction of $\vec{j}$. In the zoom the vortices (dots) and saddles (crosses) are clearly seen with their sense of rotation.

[U. Kuhl, Eur. Phys. J. Special Topics 145, 103 (2007)]

Intensity distribution (open systems)

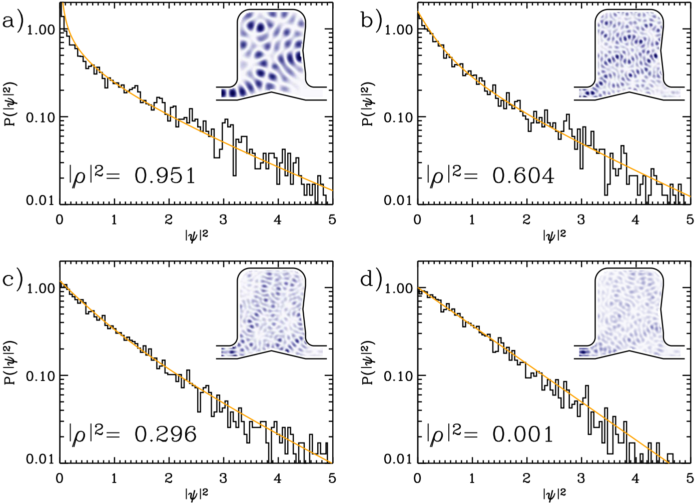

Intensity distribution for four different wave functions at frequencies $\nu = 8.0$ (a), 16.9 (b), 15.6 (c), and 15.4 GHz (d) with different phase rigidities $|\rho|^2$. The solid lines corresponds to the theoretical prediction from the RWM. The modulus of the wave function is shown in the inset.

[U. Kuhl, Eur. Phys. J. Special Topics 145, 103 (2007)]

Current distribution

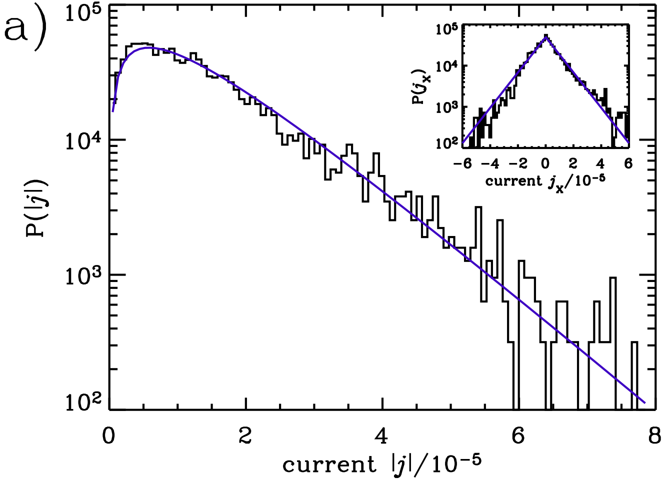

$P(|j|)$ and as an inset the x component of j ($P(j_x)$) is plotted.
The distortion for j_x comes from the main transport direction.

[U. Kuhl, Eur. Phys. J. Special Topics 145, 103 (2007)]

Vortex dynamics

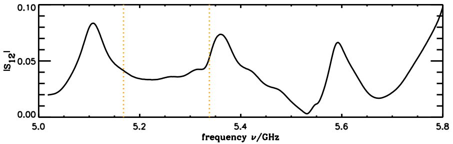

Vortices as function of frequency:
Top: Transmission $|S_{12}|$ into the billiard
Dots are vortices (clockwise: red)
Crosses are saddles (yellow)
Below: Zoom into regions of creation and annihilation

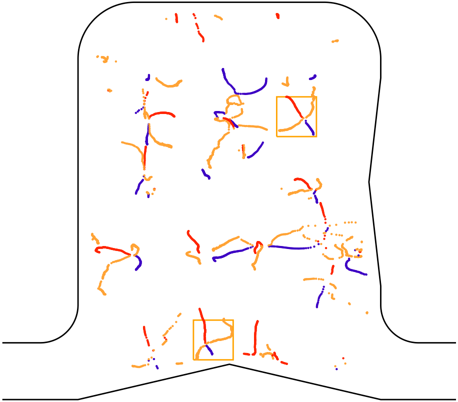

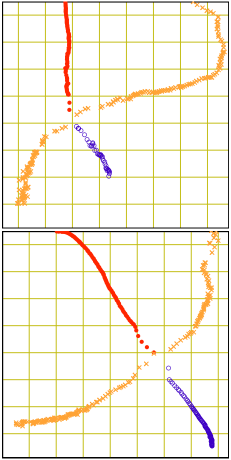

[U. Kuhl, Eur. Phys. J. Special Topics 145, 103 (2007)]

Vortex pair correlation function (theory)

Defining: $C(R) = J_0(R)$ with $R = k|\vec{r}|$ und J_0 the Bessel function. And with the following abbreviations:

$$C = C(R), E = C'(R), H = -C'(R)/R, F = -C''(R), F_0 = -C''(0)$$

$$D_1 = [E^2 - (1+C)(F_0 - F)][E^2 - (1-C)(F_0 + F)], D_2 = F_0^2 - H^2$$

$$Y = \frac{H^2(CE^2 - F(1-C^2))^2}{F_0^2(E^2 - F_0(1-C^2))^2}, Z = \frac{D_1 D_2 (1-C^2)}{F_0^2(E^2 - F_0(1-C^2))^2}$$

where $'$ denotes the derivative. Finally we can write the result as the following integral which can be evaluated numerically:

$$g_{vv}(R) = \frac{2(E^2 - F_0(1-C^2))}{\pi F_0(1-C^2)} \int_0^\infty dt \frac{3 - Z + 2Y + (3 + Z - 2Y)t^2 + 2Zt^4}{(1+t^2)^3\sqrt{1 + (1 + Z - Y)t^2 + Zt^4}}$$

The charge correlation function $g_Q(R)$ which accounts also for the chirality of the vortex points, can be expressed in a much nicer way:

$$g_Q(R) = \frac{4}{R}\frac{\mathrm{d}}{\mathrm{d}R}\left[\frac{\mathrm{d}\arcsin(J_0(R))}{\mathrm{d}R}\right]^2$$

[R. Höhmann et.al. Phys. Rev. E 79, 016203 (2009)]

Vortex pair correlation function

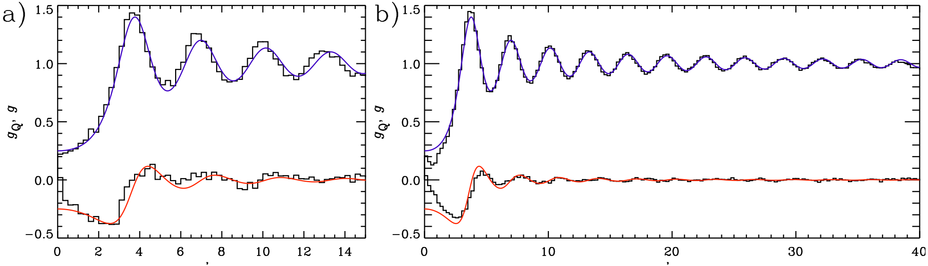

Vortex pair correlation function g and charged correlation function g_Q for low (5-9 GHz, a) and high (15-18.6 GHz b) frequencies

[R. Höhmann et al. Phys. Rev. E 79, 016203 (2009)]

Vortex nearest neighbor spacing

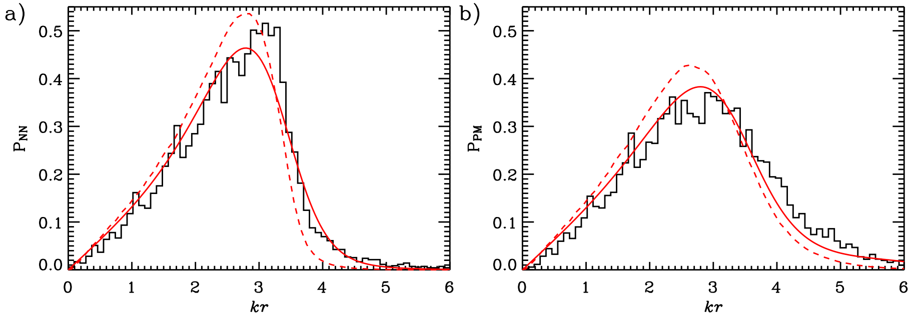

Nearest neighbor spacing for vortices without (a) and with consideration (b) of the different sense of rotation. Solid lines correspond to prediction using the Poisson approximation. Dashed lines are numerical calculations using the RWM.

[R. Höhmann et al. Phys. Rev. E 79, 016203 (2009)]

Vortex-saddle pair correlation function

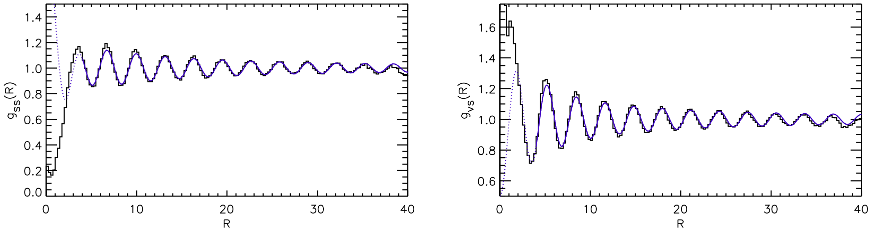

(a) Saddle-saddle correlation function $g_{\mathrm{ss}}(R)$
(b) Vortex-saddle correlations function $g_{\mathrm{vs}}(R)$
Experimental data (histogram) and asymptotic approximation

[R. Höhmann et al. Phys. Rev. E 79, 016203 (2009)]

Vortex nearest neighbor spacing

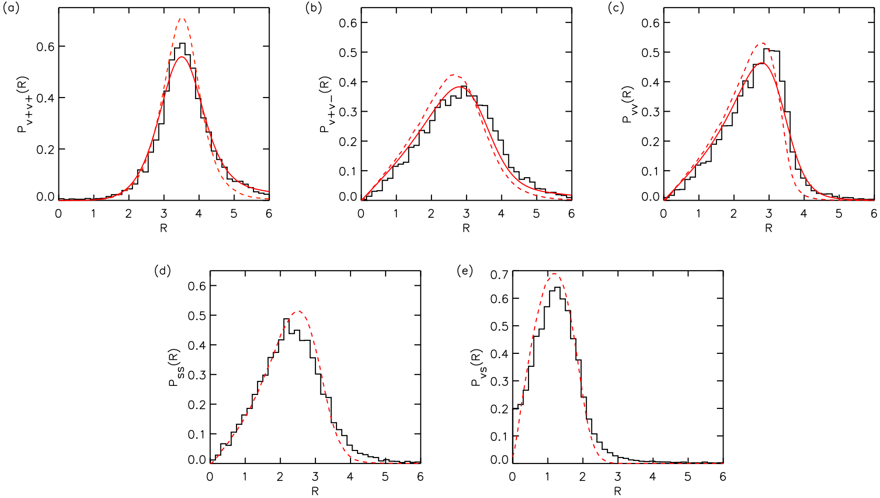

Histogramms display the different nearest neighbor spacings of critical points. Solid lines correspond to the predictions using the Poisson approximation. Dashed lines correspond to numerical calculations using the RWM. Distribution of (a) Vortices with the same, (b) different, (c) and without consideration of the sense of rotation. (d) saddle-points and (e) between vortices and saddles.

[R. Höhmann et al. Phys. Rev. E 79, 016203 (2009)]

Correlations function including size effects

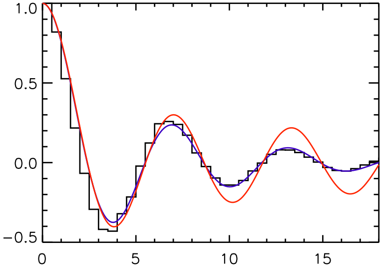

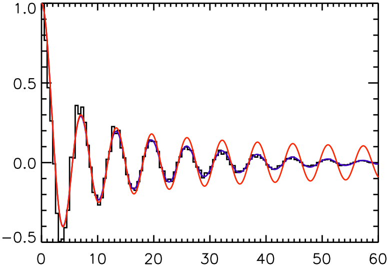

Spatial correlation function of the real part of Ψ. Left at 5.4 GHz and right at 17.96 GHz. Red line corresponds to the RWM prediction. Blue to the RWM prediction including the corrections.

Scaling factor

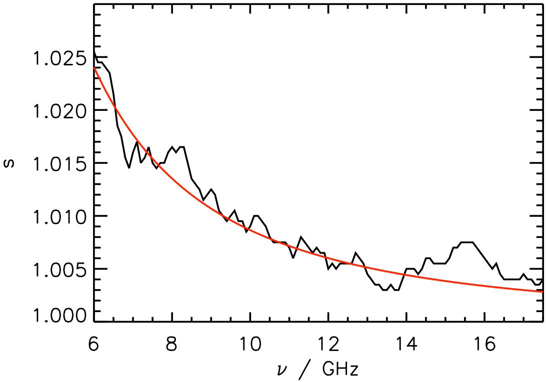

Scaling factor s for the experimental pair correlation function to reproduce the RWM prediction as a function of frequency.

Vortex density (close to a straight wall)

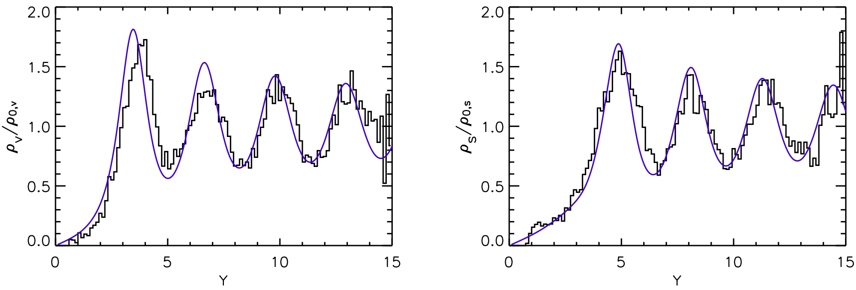

Density fluctuations of critical points as a function of the scaled distance Y from the straight wall: (left) vortex density; (right) saddle density.

[R. Höhmann et al. Phys. Rev. E 79, 016203 (2009)]